

Catalyzed CO Oxidation at 70 K on an Extended Au/Ni Surface Alloy

David L. Lahr and Sylvia T. Ceyer*

Department of Chemistry, Massachusetts Institute of Technology, Cambridge, Massachusetts 02139

Received June 12, 2005; E-mail: stceyer@mit.edu

In 1989, Haruta et al. demonstrated that Au nanoparticles supported on transition metal oxides such as TiO₂ were active for CO oxidation at 200 K.¹ The high reactivity of Au, surprising for a metal that had long been considered a catalytic dud, was attributed to sites that are formed along the perimeter of Au particles by interaction of Au with the transition metal of the support. More recently, the remarkable transformation of gold's catalytic activity was attributed to quantum size effects of Au nanoparticles or the formal oxidation state of Au atoms bound at oxygen vacancies.^{2–5} Here, we demonstrate that an extended Au surface alloy, Au/Ni(111), catalyzes low-temperature CO oxidation. No nanoscale-size Au clusters or high oxidation states of Au are present. Rather, formation of a surface alloy between Au and Ni on a Au/Ni(111) surface stabilizes adsorption of O₂ that is identified spectroscopically to be the reactant with CO at the lowest temperature known for this reaction to proceed, 70 K. These results strongly suggest that an adsorbed O₂ species similarly stabilized at the perimeter of Au nanoparticles is the critical reactant in supported oxide systems.

Gold is vapor-deposited onto a Ni(111) crystal held at 450 K and mounted in an ultrahigh vacuum chamber.⁶ Deposition of up to 0.3 ML of Au does not result in an epitaxial overlayer or islands. Instead, Au atoms randomly replace Ni atoms,^{7,8} resulting in a strongly bound surface alloy and preserving the hexagonal, two-dimensional structure of the clean Ni surface. High-resolution electron energy loss spectroscopy (HREELS) verifies the absence of contaminants such as oxygen, sulfur, and carbon. The Au coverage, measured by Auger spectroscopy, is calibrated by comparison to previous results.⁹

Saturation coverage of O₂ is adsorbed on the 0.24-ML Au/Ni surface alloy at 77 K. The vibrational spectrum, measured by HREELS, is shown in Figure 1. The dominant feature, at 865 cm⁻¹, is assigned to the O–O stretch mode of molecular oxygen whose bond axis is parallel to the surface. Similar frequencies have been observed for O₂ adsorbed on other metals,^{10–13} which have been characterized as peroxo or superoxo-like species.¹⁴ Shoulders at 790 and 950 cm⁻¹ on the 865 cm⁻¹ feature indicate molecular O₂ adsorbed at multiple sites.¹⁵ The feature at 460 cm⁻¹ is tentatively assigned to the O₂–Au/Ni stretch mode, while the feature at 320 cm⁻¹, not labeled, is a Ni phonon mode.¹⁶ Therefore, O₂ adsorption on this surface alloy is molecular. In contrast, O₂ dissociatively adsorbs on Ni(111) at a temperature as low as 8 K,¹⁷ while it adsorbs neither molecularly nor dissociatively on Au(111) at or above 100 K.¹⁸

The spectrum measured at 77 K after this layer is heated at 2 K/s to 280 K is also shown in Figure 1. The feature at 865 cm⁻¹ and its shoulders attributed to molecularly adsorbed O₂ are no longer present, and two new features at 530 and 435 cm⁻¹ appear. Specifically, the feature at 865 cm⁻¹ begins to decrease in intensity after heating to 105 K and disappears after heating to 150 K. Given the absence of O₂ desorption, this behavior is interpreted as dissociation of molecularly adsorbed O₂ into adsorbed O atoms.

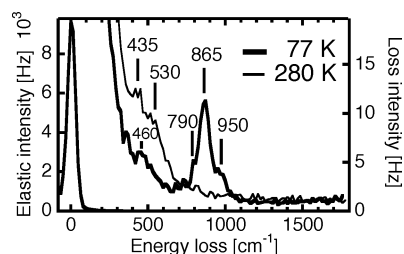


Figure 1. Specular HREEL spectrum (bold) of saturation coverage O₂ measured at 77 K on 0.24 ML of Au/Ni(111) and after heating to 280 K. Incident electron energy is 6.4 eV with 55 cm⁻¹ fwhm.

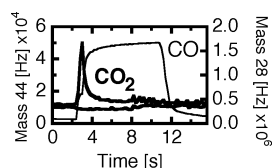


Figure 2. CO₂ (bold) and CO partial pressures, plotted as raw count rate, measured upon exposure of the O₂-covered Au/Ni alloy at 77 K to CO at 2.5 s. The reaction is largely over after 1.5 s of exposure to CO, which is incident on the O₂-covered alloy surface for 8 s. CO₂ (bold) partial pressure measured during a control experiment is also shown.

Two O–Ni stretch modes are observed. The 530 cm⁻¹ feature is assigned to O atoms bound to Ni adjacent to other Ni atoms, because this frequency is similar to that for O atoms bound to Ni(111), 580 cm⁻¹.¹⁷ The lower frequency feature at 435 cm⁻¹ is attributed to O atoms bound to Ni adjacent to Au atoms.

A beam of thermal energy CO is then directed at the O₂-covered Au/Ni(111) surface alloy held at 77 K. Production of gas-phase CO₂ coincides exactly with the introduction of CO, as shown in Figure 2 by a plot of mass 28 and 44 partial pressures as a function of time. Also shown is the mass 44 partial pressure as a function of time of CO exposure when the O₂-covered alloy surface is rotated 180°, so that the CO beam impinges on the back of the crystal mount. In this control experiment, no CO₂ is produced. This result provides clear evidence that CO reacts with molecularly adsorbed O₂ at 77 K. Experiments at 70 K indicate similar reactivity. Collision-induced desorption of O₂ by CO is not observed.^{19,20} This experiment does not distinguish between reaction of gas-phase CO with adsorbed O₂ and that of adsorbed CO with adsorbed O₂. No reaction is observed when an O₂ beam is incident on a CO-covered Au/Ni(111) alloy.

After exposure to CO, a spectrum (Figure 3) is measured. Two C=O stretch vibrational modes are observed at 2170 and 2100 cm⁻¹, along with the Au/Ni–CO stretch mode at 435 cm⁻¹. The features at 2170 and 2100 cm⁻¹ represent CO bound to Au²¹ and Ni²² atoms, respectively. The O–O mode at 950 cm⁻¹ has disappeared, while the 865 cm⁻¹ mode is greatly reduced in intensity. The decrease in intensities of these features is evidence that the molecularly adsorbed O₂ has reacted with CO to form the CO₂ shown in Figure 2. The remaining product is an adsorbed O atom, as evidenced by the appearance of a new feature at 660 cm⁻¹.

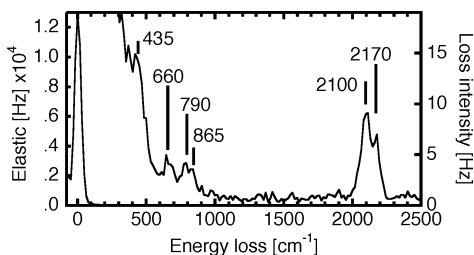


Figure 3. Specular HREEL spectrum after exposure of O₂-covered alloy at 77 K to CO beam.

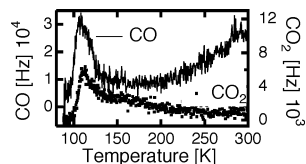


Figure 4. CO₂ and CO partial pressures versus temperature as crystal was heated at 2 K/s after exposure of O₂-covered alloy at 77 K to CO.

The O atom product is believed to be bound to a Au atom because a frequency of 660 cm⁻¹ has been observed previously for the O–Au(111) stretch mode.²³ The molecularly adsorbed O₂ that gives rise to the feature at 790 cm⁻¹ has not reacted with CO.

The alloy surface represented in Figure 3 and an O₂-covered alloy surface that has been moved out of the direct path of the CO beam are heated at 2 K/s while mass 44 and 28 partial pressures are monitored. The difference between these two traces is calculated, and then the contribution to the mass 28 signal from CO₂ dissociative ionization is subtracted from the CO trace. The results are plotted (Figure 4) as thermal desorption traces. Rapid production of gas-phase CO₂ is observed between 105 and 125 K, along with CO desorption. Production of CO₂ occurs in the same temperature range at which adsorbed O₂ dissociates. This observation suggests that CO₂ formation occurs between CO and a “hot” O atom, as proposed in cases where the temperature of CO₂ production is the same at which O₂ dissociates.²⁴ A “hot” atom is defined as an atom, produced by bond dissociation, that has not yet equilibrated with the surface. The CO desorption between 105 and 125 K is not observed in the absence of adsorbed O₂ or O. Therefore, this desorption is a consequence of weaker CO binding in the presence of adsorbed oxygen. Desorption of CO above 250 K, with a maximum desorption rate between 300 and 310 K not shown in Figure 4, is similar to that observed in the absence of adsorbed oxygen. The high CO desorption rate relative to CO₂ production is a consequence of the reaction conditions of excess CO.

Above 125 K, CO₂ is produced slowly. A vibrational spectrum measured after raising the temperature to 280 K shows that the O feature at 660 cm⁻¹ and the CO feature at 2170 cm⁻¹ have disappeared, suggesting that the CO and adsorbed O atoms that react above 125 K are bound to Au atoms. The intensity of the CO feature at 2100 cm⁻¹ remains undiminished after heating to 280 K. Adsorbed O atoms bound to Ni atoms are also present after heating to 280 K, as indicated by the presence of weak intensity between 435 and 530 cm⁻¹. The small amount of remaining adsorbed oxygen is not surprising given that adsorbed oxygen is the limiting reactant under the conditions of these experiments. No O₂ is observed to desorb. Heating the surface to 900 K results in no additional CO₂ desorption. Exposure of the alloy surface covered with atomically adsorbed oxygen, represented by the spectrum labeled 280 K in Figure 1, to CO does not result in reaction at any

temperature. That is, O atoms adsorbed on Ni atoms and identified by the 435–530 cm⁻¹ features are unreactive with CO. The surface structure of Au/Ni is not perturbed by CO or O₂.²⁵

These results demonstrate that Au/Ni(111) catalyzes CO oxidation at low temperature by at least three distinct mechanisms. At the lowest temperature, 70 K, O₂ is the reactant with CO. Given an O₂ coverage of no more than 0.5 ML, an incident CO flux of about 0.5 ML/s, and completion of the reaction at 70 or 77 K in about 1 s, the reaction probability of CO with molecularly adsorbed O₂ is estimated to be between 0.5 and 1. The necessity of a molecularly adsorbed species, as opposed to gas-phase O₂, for reaction with CO is clear from the absence of reactivity upon exposure of the CO-covered surface alloy to a beam of O₂. Between 105 and 125 K, CO₂ production coincides with O₂ dissociation, suggesting a “hot atom” mechanism. Above 125 K, CO bound to Au atoms reacts with O atoms bound to Au atoms.

Interestingly, density functional calculations of CO oxidation on Au nanoclusters supported on TiO₂²⁶ and MgO²⁷ reveal that an adsorbed O₂⁻² peroxy species is the key reactant in CO oxidation. It is bound to Ti or Mg atoms adjacent to a Au nanocluster and provides a low energy pathway for transfer of an oxygen atom to CO weakly adsorbed on the Au nanocluster. Recently, an experiment suggested that a reactant for CO oxidation on supported Au clusters might be O₂.²⁸

Acknowledgment. This work was supported by DoE, DE-FG02-05ER15665.

References

- (1) Haruta, M.; Yamada, N.; Kobayashi, T.; Iijima, S. *J. Catal.* **1989**, *115*, 301–309.
- (2) Valden, M.; Lai, X.; Goodman, D. W. *Science* **1998**, *281*, 1647–1650.
- (3) Gudman, J.; Gates, B. C. *J. Am. Chem. Soc.* **2004**, *126*, 2672–2673.
- (4) Yoon, B.; Hakkinen, H.; Landman, U.; Worz, A. S.; Antoniette, J. M.; Abbet, S.; Judai, K.; Heiz, U. *Science* **2005**, *307*, 403–407.
- (5) Chen, M. S.; Goodman, D. W. *Science* **2004**, *306*, 252–255.
- (6) Ceyer, S. T.; Gladstone, D. J.; McGonigal, M.; Schulberg, M. T. In *Physical Methods of Chemistry*, 2nd ed.; Rossiter, B. W., Baetzold, R. C., Eds.; Wiley: New York, 1993; Vol. IXA, pp 383–452.
- (7) Jacobsen, J.; Nielsen, L. P.; Besenbacher, F.; Stensgaard, I.; Laegsgaard, E.; Rasmussen, T.; Jacobsen, K. W.; Nørskov, J. K. *Phys. Rev. Lett.* **1995**, *75*, 489–492.
- (8) Umezawa, K.; Nakanishi, S.; Gibson, W. M. *Phys. Rev. B* **1998**, *57*, 8842–8844.
- (9) Holmblad, P. M.; Larsen, J. H.; Chorkendorff, I. *J. Chem. Phys.* **1996**, *104*, 7289–7295.
- (10) Gland, J. L.; Sexton, B. A.; Fisher, G. B. *Surf. Sci.* **1980**, *95*, 587–602.
- (11) Backx, C.; de Groot, C. P. M.; Biloen, P. *Surf. Sci.* **1981**, *104*, 300–317.
- (12) Imbihl, R.; Demuth, J. E. *Surf. Sci.* **1986**, *173*, 395–410.
- (13) Sueyoshi, T.; Sasaki, T.; Iwasawa, Y. *Surf. Sci.* **1996**, *365*, 310–318.
- (14) Gravil, P. A.; Bird, D.; White, J. A. *Phys. Rev. Lett.* **1996**, *77*, 3933–3936.
- (15) Ibach, H. *J. Vac. Sci. Technol.* **1982**, *20*, 574–577.
- (16) Ibach, H.; Bruchmann, D. *Phys. Rev. Lett.* **1980**, *44*, 36–39.
- (17) Beckerle, J. D.; Yang, Q. Y.; Johnson, A. D.; Ceyer, S. T. *Surf. Sci.* **1988**, *195*, 77–93.
- (18) Légaré, P.; Hilaire, L.; Sotto, M.; Maire, G. *Surf. Sci.* **1980**, *91*, 175–186.
- (19) Beckerle, J. D.; Johnson, A. D.; Ceyer, S. T. *Phys. Rev. Lett.* **1989**, *62*, 685–688.
- (20) Beckerle, J. D.; Johnson, A. D.; Ceyer, S. T. *J. Chem. Phys.* **1990**, *93*, 4047–4065.
- (21) Ruggiero, C.; Hollins, P. *Surf. Sci.* **1997**, *377*–379, 583–586.
- (22) Tang, S. L.; Lee, M. B.; Yang, Q.; Beckerle, J. D.; Ceyer, S. T. *J. Chem. Phys.* **1986**, *84*, 1876–1883.
- (23) Pireaux, J. J.; Liehr, M.; Thiry, P. A.; Delrue, J. P.; Caudano, R. *Surf. Sci.* **1984**, *141*, 221–232.
- (24) Matsushima, T. *Surf. Sci.* **1983**, *127*, 403–423.
- (25) Nielsen, L. P. Ph.D. Thesis, University of Aarhus, Aarhus, Denmark, 1996.
- (26) Liu, Z.-P.; Gong, X.-Q.; Kohanoff, J.; Sanchez, C.; Hu, P. *Phys. Rev. Lett.* **2003**, *91*, 266102-1-4.
- (27) Molina, L. M.; Hammer, B. *Phys. Rev. B* **2004**, *69*, 155424-1-22.
- (28) Stiehl, J. D.; Kim, T. S.; McClure, S. M.; Mullins, C. B. *J. Am. Chem. Soc.* **2004**, *126*, 13574–13575.

JA053866J